Journal of Electronic Materials (2023) 52:5642–5651
https://doi.org/10.1007/s11664-023-10509-4

ORIGINAL RESEARCH ARTICLE

Growth, Spectral, Optical, Mechanical, Thermal, Magnetic, Impedance, and Nonlinear Optical Properties of L-Alanine Nickel Chloride Crystal

S. Thangavel[1] · V. Kathiravan[2] · R. Ashok Kumar[1] · T. Muthu Lakshmi[2] · G. Satheesh Kumar[3] · P. Selvarajan[4] · M. Kumaresavanji[5]

Received: 19 December 2022 / Accepted: 10 May 2023 / Published online: 1 June 2023

Abstract

A semi-organic nonlinear optical crystal of L-alanine nickel chloride (LAN) has been successfully grown by a slow evaporation solution method. The single-crystal x-ray diffraction technique determined the lattice parameters of the crystal. Fourier-transform infrared spectral analysis confirmed the functional groups present in the crystal lattice. The crystal was subjected to UV–Visible-NIR transmittance measurements, and its band-gap energy was determined using transmittance studies. A Nyquist plot was used to determine the crystal's bulk resistance and dc conductivity. Fluorescence analysis was performed on the crystal, and green visible light was emitted from it when it was excited by UV light. Microhardness measurements were made on the crystal, and numerous parameters were analyzed. We studied the crystal's nonlinear optical properties, while its magnetic properties were determined using a vibrating sample magnetometer. TGA/DTA analysis was performed on the crystal, and it was found that its Second-harmonic Generation efficiency was more than that of the standard KDP sample. Hence, this crystal could be useful in laser technology, optical communication, optical computing, optical data processing, and photonics.

Keywords X-ray diffraction · fluorescence · nonlinear optical material · impedance · magnetic property

Introduction

Nonlinear optical (NLO) materials are commonly used in optical modulation, fiber-optic communication, and opto-electronics.[1,2] Over the last decade, organics have dominated the quest for novel frequency conversion materials. However, organic crystals have extremely broad nonlinear susceptibilities compared to inorganic crystals. According to recent research, their use is limited by their low optical transparency, poor mechanical properties, low thresholds for laser damage, and inability to produce and process large crystals. Due to the absence of extended-electron delocalization, pure inorganic NLO materials usually exhibit superior mechanical and thermal properties but also exhibit mild optical nonlinearity. In semi-organic crystals, polarizable organic molecules are stoichiometrically bound within the organic host.[2] Semi-natural systems offer countless frameworks and plans for the sub-atomic construction of new materials in crystal design techniques for assembling materials. "Semi-organic NLO materials are ideal for system manufacturing technology due to their improved chemical and physical properties, including high thermal stability, excellent mechanical hardness, wide nonlinear coefficient, wide optical frequency range, and laser-induced resistance."[3–5] Semi-organic materials are coordination complexes of metals with organic ligands in which the organic ligand plays a prominent role in the NLO effect. Recent efforts have been undertaken to combine amino acids with novel inorganic

✉ V. Kathiravan
vkathiravan75@gmail.com

1 PG and Research Department of Physics, Thiruvalluvar Government Arts College, Rasipuram, Tamilnadu 637401, India

2 Crystal Growth Laboratory, PG and Research Department of Physics, Government Arts, College (Autonomous), Karur, Tamilnadu 639005, India

3 Department of Science and Humanities, Nehru Institute of Technology, Kaliapuram, Coimbatore, Tamilnadu 641105, India

4 Department of Physics, Aditanar College of Arts and Science, Tiruchendur, Tamil Nadu 628216, India

5 PG and Research Department of Physics, National College (Autonomous), Tiruchirappalli, Tamilnadu 620001, India

materials to generate materials superior to existing ones. The Zwitterionic shape alters amino acids' physical and chemical characteristics.[6–9]

"Amino acids are fascinating materials for NLO application as they contain proton benefactor carboxyl acid (−COO) group and the proton acceptor amino (NH_2) group in them."[10–13] L-alanine is an excellent organic nonlinear optical material belonging to the amino acid category, with a melting point of 297°C and belonging to the orthorhombic crystal system with a space group of $P2_12_12_1$. L-alanine, with a molecular weight of 89.09, is one of the smallest naturally occurring chiral amino acids.[14–18] Many scholars have investigated L-alanine complex crystals and published their findings.[19–22] L-alanine is an organic material, and nickel chloride is an inorganic material; hence these chemicals have been mixed in a 1:1 molar ratio to produce a semi-organic NLO crystal, namely L-alanine nickel chloride (LAN). Here, I is intended to react nickel chloride with L-alanine and change the different properties of L-alanine. The advantages and disadvantages of organic and inorganic chemicals are considered in this investigation. It is known that an organic NLO crystal like L-alanine has low thermal stability, low mechanical strength, and high second-harmonic generation (SHG) efficiency, and an inorganic crystal like nickel chloride has high thermal stability, high hardness, and low NLO response; hence, the organic and inorganic reactants have been mixed to form a semi-organic NLO crystal. This paper aims to report the LAN crystal's growth, thermal, mechanical, electrical, magnetic, and optical properties, and SHG efficiency.

Experimental

Material Preparation and Crystal Growth

The purity of source materials such as L-alanine and nickel chloride was 99%, and the chemicals were of AR grade, purchased from Merck India. L-alanine and nickel chloride were taken in an equimolar ratio. L-alanine in the estimated quantity was first dissolved in double-distilled water, then, nickel chloride was slowly added to the solution by stirring for 5 h at room temperature.[18] The salt was obtained using a slow evaporation method after the prepared solution was allowed to dry at room temperature. Re-crystallization was used to increase the purity of the synthesized salt. After 23 days of growth, a transparent whitish-green colored crystal was obtained. Since the title crystal is soluble in water, the high optical quality crystal of L-alanine nickel chloride (LAN) was grown by aqueous solution with slow evaporation. As this sample decomposes before melting, the melting method could not be adopted to grow the crystal. Processing methods, such as stirring and filtering, were performed during the preparation of the solution. The crystal's image is shown in Fig. 1, and the size of the crystal was $20 \times 15 \times 11$ mm^3.

Fig. 1 A grown LAN crystal.

Table I Lattice parameters value of the LAN crystal

Cell parameters (Å)			Volume (Å^3)	System
a	*b*	*c*		Orthorhombic
8.530	7.156	8.564	522.753	[$\alpha = \beta = \gamma = 90°$]

Results and Discussion

Single-Crystal X-ray Diffraction Analysis

The crystal of LAN was a single crystal; hence, we carried out a single-crystal x-ray diffraction study (XRD; Kappa Apex-II single crystal diffractometer, equipped with MoK_α radiation ($\lambda = 0.7101$ Å); Bruker) to find the crystal structure and lattice parameters. The lattice parameter values of the crystal are tabulated in Table I.

It was found that the lattice parameters of the crystal are completely different than those of the L-alanine crystal[22]; hence, a new compound of LAN has been formed, and this work is reported for the first time.

Fourier-Transform Infrared (FT-IR) Vibrational Spectroscopic Studies

The FT-IR spectrum of the grown LAN crystal was recorded at room temperature using the KBr pellet technique on a Perkin Elmer Spectrometer in the range of 4000–500 cm^{-1} (Fig. 2).

The absorption peak at 3452 cm^{-1} occurring in the higher energy region is due to the N-H stretch of the NH_3^+ symmetric stretching mode of vibration. At 3006 cm^{-1}, the CH_2 symmetric stretching vibration mode emerged. Vibrations in the C-H stretching mode were detected at 2923 cm^{-1} and 2592 cm^{-1}. In the crystal, the carboxylic

group was detected as COO^-, and an ionized carboxylic group was detected in the region of 1413–1112 cm^{-1}.

The vibration peak at 2249 cm^{-1} is due to CH_3 stretching, but the transmission peaks detected at 1583 cm^{-1} and 1509 cm^{-1} are due to the ammonium group (NH_3^+ bending). The vibration peak at 2113 cm^{-1} is due to the torsional oscillation of NH_3^+. The C-O stretching mode of vibration was observed at 1740 cm^{-1}. The vibration peak observed at 1013 cm^{-1} is attributed to the overtone of the torsional oscillation of NH_3^+. At 848 cm^{-1}, the C-C-N stretching mode of vibration was detected. The O-C-O bending mode at 771 cm^{-1} was identified. The COO^- scissoring and COO^- rocking mode of vibrations were observed at 649 cm^{-1} and 536 cm^{-1}, respectively.[18] Table II shows the frequency assignment of multiple functional groups found in the LAN crystal.

Optical Properties

Linear Optical Transmission Study and the Relevant Constants

Optical measurement techniques such as spectroscopy are useful for determining the optical properties of crystals. In most cases, these methods are non-destructive, making them suitable for measuring optical parameters. Materials' optical properties are essential in assessing their suitability for optoelectronic devices. "The optical properties of a crystal are primarily determined by its optical transparency, absorption coefficient, band gap, extinction coefficient, and refractive index."[23] The interaction of the crystal with the electric and magnetic fields produced by the electromagnetic wave determines the crystal's optical properties. To investigate a material's possible optoelectronic applications, it is essential to be familiar with optical constants such as the optical band gap and extinction coefficient. Additionally, materials' optical properties can be related to their atomic structure, electrical properties, and electronic band structure.

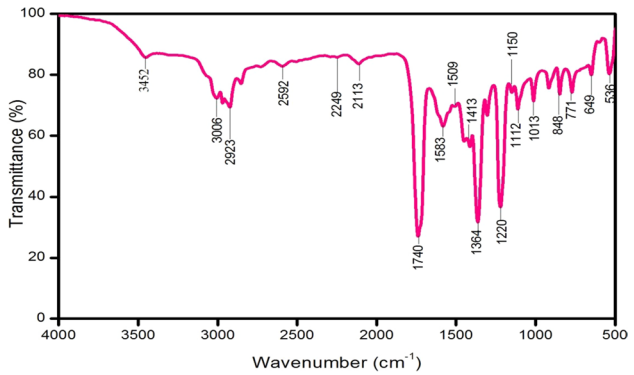

Fig. 2 FT-IR spectrum of the LAN crystal.

Table II FT-IR spectral assignments for LAN crystal

Wavenumber (cm^{-1})	Assignments
3452	NH_3^+ symmetric stretching
3006	CH_2 asymmetric stretching
2923,2592	C-H stretching
2249	CH_3 stretching
2113	NH_3^+ torsion
1740	C = O stretching
1583,1509	NH_3^+ bending
1413—1112	COO^- symmetric stretching
1013	An overtone of torsional oscillation of NH_3^+
848	C-C-N stretching
771	O-C-O deformation
649	COO^- scissoring
536	COO^- rocking

Optical Band Gap

The UV–Vis-NIR transmittance spectrum was measured using a Perkin-Elmer Lambda 35 Spectrometer over the wavelength range 190–1100 nm. Optical transmittance research is beneficial for determining the optical transmission range of a crystal's cut-off wavelength. When light interacts with a molecule, it is often important to understand its electronic transition states. Figure 3 shows the UV–Vis-NIR spectrum of the LAN crystal that was observed. The wavelength of the lower cut-off for the sample was 245 nm which is the same as the lower cut-off wavelength of the L-alanine crystal,[24] while an extra absorption peak at 265 nm appears in the case of the LAN crystal. The high transmittance of the LAN crystal in the range from 300 nm to 1100 nm is very good for the emission of SHG radiation and other NLO applications.[25]

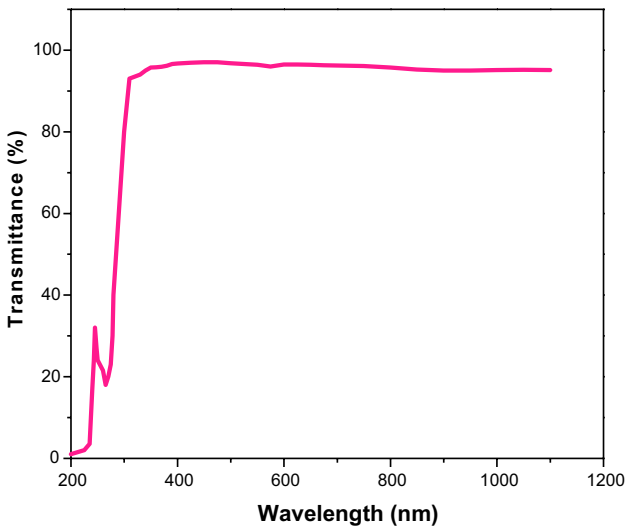

Fig. 3 UV–Vis- NIR spectrum of the LAN crystal.

Due to the COO^- and NH_2 groups' presence, limited conjugation length, and solid resonance in the crystalline state of LAN, the spectrum shows excellent transparency in the entire visible region of 400–800 nm. The magnitude of the optical energy band gap is one of the main goals of this research. The band gap (E_g) was computed to be 5.06 eV using the formula $E_g = 1240/\lambda$ (here, λ is the wavelength in nanometers).

Optical transmittance measurements at room temperature were used to obtain the absorption coefficient (α) of the LAN crystal. The value was calculated using:

$$\alpha = \frac{2.303 \log (1/T)}{t} \quad (1)$$

where T and t are the sample's transmittance and thickness, respectively. The relationship between the absorption coefficient (α) and the photon energy ($h\nu$) is:

$$(\alpha h\nu)^2 = A\left(h\nu - E_g\right) \quad (2)$$

where E_g is the crystal's optical band gap, and A is a constant. "A plot (Fig. 4) is drawn using the above relation, and the optical band gap is found to be 5.10 eV" and this value is observed to be almost the same as that of L-alanine.[23–34]

Luminescence Studies

Fluorescence is the emission of light that stops after the source of excitation has been cut off, and is most commonly seen in organic molecules with a rigid framework. The excitation wavelength used in this work was 240 nm. The nature of the sample used in the fluorescence study was the cut and polished crystal of LAN. The fluorescence emission spectrum was measured using a Perkin Elmer fluorescence spectrofluorometer in the range of 490–570 nm and is shown in Fig. 5. The emission spectra show a peak at 528 nm, demonstrating a green fluorescence emission.[35]

Since the sample is slightly green in color, the LAN crystal emits green light when it is excited with UV light of a wavelength of 240 nm.

Second-Harmonic Generation (SHG) Studies

"SHG is also known as frequency doubling in nonlinear optics. It happens when photons interact successfully with a nonlinear material to form new photons with twice the energy and twice the original photons' frequency." The Kurtz and Perry powder approach was used to determine the SHG conversion efficiency of LAN.[36] The crystal was ground into a uniform powder before being placed in a microcapillary tube, and then passed through an Nd:YAG laser (λ = 1064 nm) with a pulse length of 6 ns. A standard potassium dihydrogen phosphate (KDP) crystal was used as the reference sample. The SHG behavior was validated by the output of the green-light-emitting laser beam. For the input energy of 0.65 J, the LAN crystal produced a second-harmonic emission of 20 mV, while the standard KDP crystal produced an SHG of 17 mV for an equal input energy. As a result, the cultivated LAN crystal has an SHG efficiency of 1.17 times that of the standard KDP crystal. For comparison purposes, the relative SHG efficiency of some of the L-alanine-based crystals are provided in Table III. It can be seen that the SHG efficiency of the L-alanine nickel chloride crystal is compared with other L-alanine-based crystals. Since the LAN crystal has a relative SHG efficiency of more than 1, it can be used for NLO, photonic, optical communication, and laser applications.

Microhardness Measurement

Vickers microhardness studies were carried out to investigate the LAN crystal's mechanical behavior using a Shimadzu HMV-2 Vickers microhardness tester. "The strength,

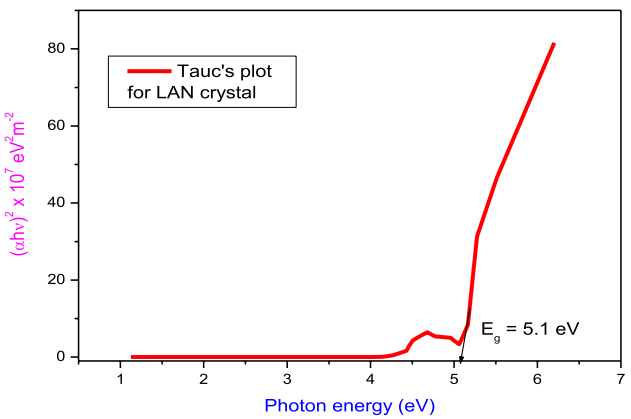

Fig. 4 Plot of $(\alpha h\nu)^2$ versus $h\nu$ of the LAN crystal.

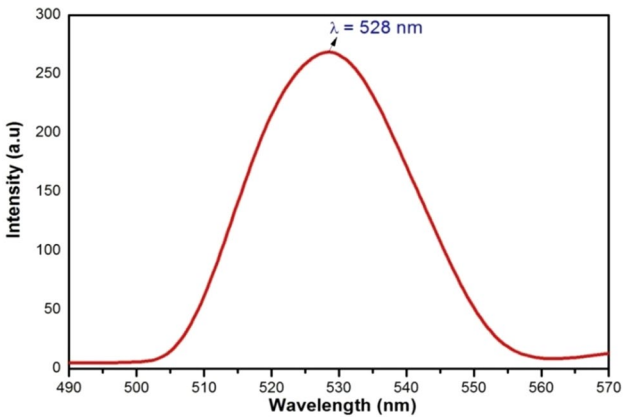

Fig. 5 Fluorescence spectrum of LAN crystal.

Table III Relative SHG efficiency of some L-alanine-based crystals

S. no	Name of the crystal	Relative SHG efficiency	Reference number
1	L-alanine nickel chloride	1.17	Current study
2	L-alanine strontium chloride trihydrate	1.4	[18]
3	L-alanine formate	2	[21]
4	L-alanine hydrogen chloride	0.76	[22]
5	L-alanine sodium nitrate	2	[37]
6	L-alanine alaninium picrate	1.47	[38]
7	L-alanine	0.33	[39]

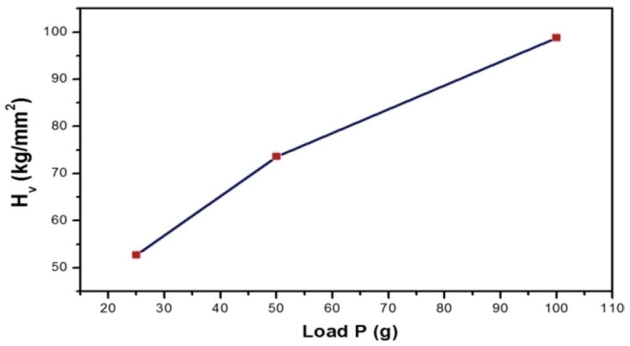

Fig. 6 Variation of H_v with applied load P for the LAN crystal.

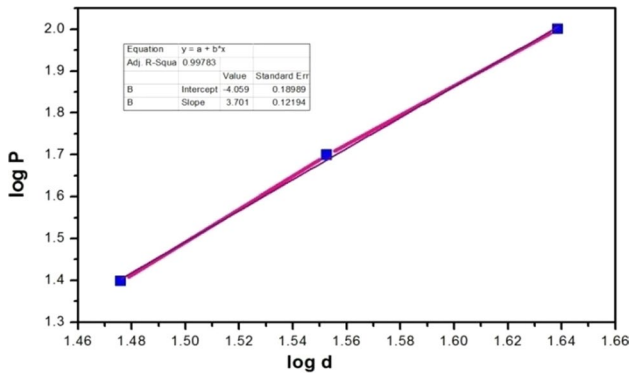

Fig. 7 Plot of log P versus log d for the LAN crystal.

molecular bindings, yield strength, and stiffness constant of a crystal are determined by its hardness."[40–42] Hardness is a mechanical property of solids that is heavily influenced by their structure and composition. It is sometimes characterized as resistance to dislocation motion, deformation, or damage under applied stress.[43] The cut and well-polished crystals were subjected to a static indentation test with a load ranging from 25 to 100 g at room temperature. For loading, the indentation time was maintained at 10 s. At least five well-defined impressions were found for each load, and the average of all the diagonals (d) was computed.

The Vickers microhardness value (Hv) was obtained from:

$$H_v = 1.8544\frac{P}{d^2}\text{kg/mm}^2 \tag{3}$$

where P denotes the applied load in g, d denotes the diagonal length of the impression in mm, and 1.8544 is a constant of the geometrical factor for the diamond pyramidal indenter. The relationship between hardness number (H_v) and load (P) for the LAN crystal is shown in Fig. 6.

The crystal's hardness increases as the load increases, and, above 100 g, cracks occur on the smooth surface due to the release of internal stresses caused by the indentations.[44] Meyer's law $P = ad^n$ describes the relationship between load and indentation size. The constants a and n vary depending on the material.[44]

The work-hardening coefficient n was determined to be 3.701 by graphing log P versus log d (Fig. 7). "According to Onitsch and Hanneman, the value of 'n' for hard materials is between 1 and 1.6, whereas 'n' for soft materials is greater than 1.6."[39,45] As a result, it has been assumed that the LAN crystal is a substance of the soft group.

Yield Strength (σ_y)

The yield strength of the grown LAN crystal can also be calculated using the relationship:

$$\sigma_y = \frac{H_v}{3}\text{N/m}^2 \tag{4}$$

where H_v represents the hardness of the material and σ_y is the yield strength.

As illustrated in Fig. 8, a graph is plotted between yield strength and load. The yield strength increases as the load increases, implying that the LAN crystal has a comparatively high mechanical strength.

Elastic Stiffness Constant (C_{11})

"The elastic stiffness constant is a measure of a material's ability to resist deformation and indicates how tightly atoms are bound together."[46] The elastic stiffness constant for different loads was computed using Wooster's empirical formula:

$$C_{11} = \left(H_v\right)^{7/4} \mathrm{N/m^2} \tag{5}$$

The variation of C_{11} with the load is depicted in Fig. 9.

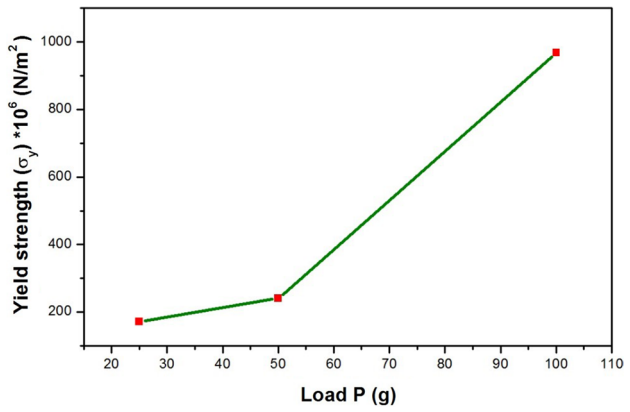

Fig. 8 Variation of yield strength with a load of LAN crystal.

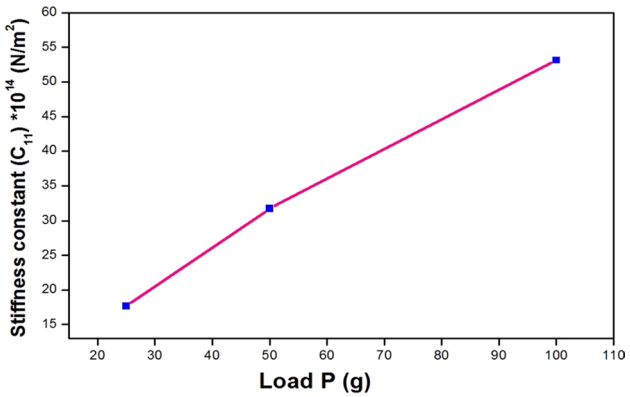

Fig. 9 Variation of stiffness constant with load for the LAN crystal.

As shown in Fig. 9, the stiffness constant increases as the load increases. When the stiffness constant is high, the ion-ion binding forces are extremely strong.

Fracture Toughness (K_c)

The fracture toughness was determined by:

$$K_c = \frac{P}{\beta C^{3/2}} \mathrm{Kg\ mm^{-3/2}} \tag{6}$$

where C is the crack circumference from the indentation mark's center to the crack tip, P denotes the applied load, and $\beta = 7$ is the Vickers indenter's geometrical constant.

Brittleness Index (B_I)

The formula for calculating the brittleness index (B_I) is:

$$B_I = \frac{H_v}{K_c} \tag{7}$$

Brittleness is another natural property that influences a material's mechanical behavior and determines whether it can fracture without significant deformation. For multiple loads (P), the hardness (H_v), stiffness constant (C_{11}), yield strength (σ_y), fracture toughness (K_c), and brittleness index (B_I) have been calculated and are described in Table III. It has been found from the microhardness study that mechanical properties like hardness, elastic stiffness constant, yield strength, fracture toughness, and the brittleness index of the LAN crystal are high, and hence it can be used for NLO device fabrication. Since the mechanical properties of the sample are high, the thermal stability the LAN crystal are also high, as per the result obtained from thermogravimetric (TGA) and differential thermal analysis (DTA) studies (Table IV).

Thermal Analysis (TGA/DTA)

TGA/DTA analysis was performed using a NETZCH STA449F3 thermal analyzer at the heating rate of 10 °C/min in the temperature range of 25–450 °C in a nitrogen environment. The thermograms of the LAN crystal are shown in Fig. 10. The TGA curve demonstrates no weight loss up

Table IV Calculated mechanical parameters of the LAN crystal

Load P (g)	H_v (kg mm^{-2})	Stiffness constant (C_{11}) (× 10^{14} N/m^2)	Yield strength (σ_y) (× 10^6 N/m^2)	Fracture toughness K × 10^5 (kg mm$^{-3/2}$)	Brittleness index B_I × 10^{-5}
25	52.7	17.69	172.15	21.318	2.47
50	73.6	31.74	240.42	42.63	1.72
100	98.8	53.14	968.24	85.27	1.15

to 244 °C, indicating that the LAN crystal is stable at that temperature. A high endothermic peak at 293 °C in the DTA range corresponds to the material's melting point. The sharp endothermic peak indicates that the sample has a high degree of crystallinity.[47,48]

It was determined from the thermal analysis results that no transformation or weight loss occurred below 244 °C. As a result, the LAN crystal can be used in various applications up to 244 °C.

Impedance Analysis

The impedance analysis for the LAN crystal was carried out in the frequency range of 1 Hz to 1 MHz at room temperature, using an impedance analyzer (STAT MC; Versa). $Z^* = Z'\text{-}jZ''$ represents a material's frequency-dependent electrical properties in terms of its complex impedance (Z^*), where Z' and Z'' indicate the real and imaginary components of impedance, respectively, and j represents the imaginary factor.[49] The sample was powdered and then pelletized, and the thickness of the pellet used in the study was 1.72 mm. For getting a good ohmic contact during the impedance measurement, both sides of the pellet were coated with the good-quality silver paint.

Figure 11 depicts the Nyquist plot of the LAN crystal at room temperature. A semicircular arc can be seen, implying that bulk effects dominate the material's electrical characteristics,[50] which determines the crystal's bulk resistance, which was 15,461 Ω**.** The dc conductivity (σ_{dc}) of the LAN crystal was determined by:

$$\sigma_{dc} = \frac{d}{AR_b}\Omega^{-1}\mathrm{m}^{-1} \tag{8}$$

where d denotes the crystal's thickness, A is the crystal surface area, and R_b is the bulk resistance of the crystal. The LAN crystal's dc conductivity was found to be 2.467×10^{-6} Ω^{-1} m^{-1} at room temperature. The crystal's low direct current conductivity is due to a decrease in charge carrier mobility caused by the ion size, which results in major changes in the electronic band structure.[51,52]

Magnetic Property–Ferromagnetic Behavior

The magnetic properties of the LAN crystal were investigated using a vibrating sample magnetometer (VSM) (7404; Lakeshore) at room temperature. The sample was collected as a fine powder.

The magnetization of the LAN crystal as a function of the applied magnetic field at room temperature is plotted in Fig. 12. The S-shaped curve in the center region of the plot suggests that the material exhibits ferromagnetic ordering during magnetization. According to the hysteresis curve depicted in Fig. 12, the LAN crystal's coercivity and remanence have been measured to be 139.841 Oe and 2.3007×10^{-7} emu/g, respectively. These values are presented in Table V.

A slight decrease in magnetization was observed above the saturation value. This may be due to a reduction in the spin–exchange interaction as the applied field increases. The saturation magnetization was found to be 1.0416×10^{-6} emu/g . The plot explicitly depicts the crystal's ferromagnetic behavior. The material is described as a soft magnetic material due to the steepness of the loop's shape. Because the loop has a smaller area, the hysteresis loss is still small. The squareness ratio (M_r/M_s) was also estimated, and the small value of M_r/M_s suggests a magnetostatic interaction with multigrains. When pure L-alanine was put perpendicular to a magnetic field, it was a diamagnetic material, while the diamagnetic behavior was unexpectedly altered to a ferromagnetic behavior, as evidenced by VSM measurements.

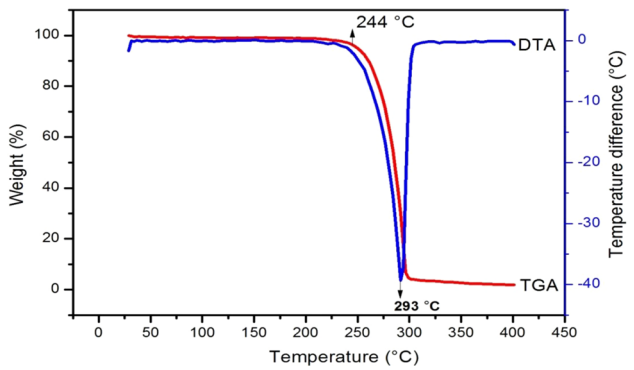

Fig. 10 TGA/DTA thermogram of the LAN crystal.

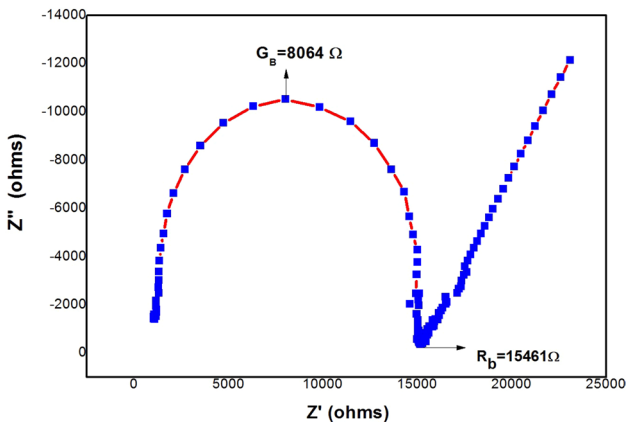

Fig. 11 Nyquist plot for the LAN crystal.

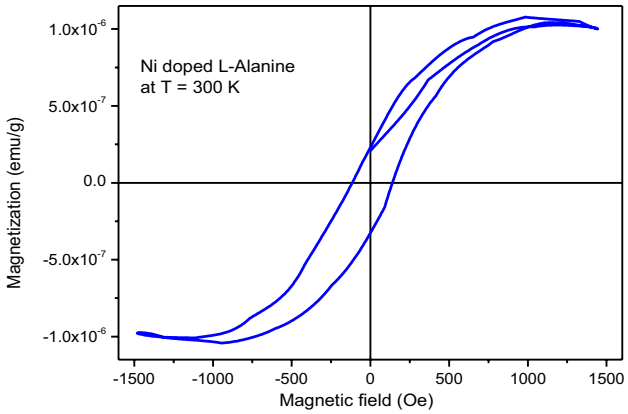

Fig. 12 Plot of magnetization versus magnetic field for the LAN crystal.

Table V Magnetic parameters of the LAN crystal

Saturation magnetization (M_s) (emu/g)	Remanence (M_r) (emu/g)	Coercivity H_C (Oe)	Squareness ratio (M_r/M_s)
1.0416×10^{-6}	2.3007×10^{-7}	139.841	0.221

Conclusion

An NLO crystal, i.e., L-alanine nickel chloride (LAN), was harvested after a growth period of 3 weeks by the solution method. XRD examination of a single crystal showed that the LAN crystal was orthorhombic. The vibrational modes of the functional group were confirmed by FT-IR spectral analysis. According to optical property tests, the crystal had a very high transmission across the entire visible field, which is the most attractive property of the material-processing NLO operation. The band-gap energy of the crystal was evaluated by UV–visible spectral study. According to the fluorescence spectrum, LAN emits a green fluorescence at 528 nm. Vickers microhardness tests were used to assess the mechanical strength of the crystal. Nonlinear optical experiments confirmed the SHG property. The crystal was stable up to 244 °C, as determined by thermal analysis. The crystal's dc conductivity was measured using a Nyquist plot. The coercivity and remanence of the crystal were calculated from the hysteresis curve as 139.841 Oe and 2.3007×10^{-7} emu/g, respectively. The relative SHG efficiency of the LAN crystal was 1.17 times that of a KDP sample. Since the crystal of LAN had a high thermal stability, high hardness, high NLO property, high transparency, and high optical band gap, this sample can be used for NLO devices, such as second-harmonic generators, third-harmonic generators, sum-frequency generators, laser devices, and photonic devices, and could also be used for optical communication, optical data processing and optical computing.

Acknowledgments The authors are grateful for the support from various research centers such as the SAIF- IIT, Madras, ACIC—St. Joseph's College, Tiruchirappalli, NCIF—National College, Tiruchirappalli and Alagappa University, Karaikudi. The authors would like to acknowledge the support extended to this research by APRC—Sacred Heart College, Tirupattur, CIF—Pondicherry University, Pondicherry, and IISC -Bangalore for their full-fledged support in carrying out characterization measurements.

Author Contribution ST, VK, RAK, TML, GSK, PS, MK: Conceived and designed the experiments; Performed the experiments; Analyzed and interpreted the data; Contributed reagents, materials, analysis tools, or data; Wrote the paper.

Funding This research did not receive any specific grant from funding agencies in the public, commercial, or not–for–profit sectors.

Conflict of interest The authors declare no conflict of interest.

References

1. S.R. Marder, L.V. Interrante, and L.A. Casper eds., *Materials Chemistry: An Emerging Discipline*. (Washington D. C.: ACS Press, 1995).
2. P.N. Prasad and D.J. Williams, *Introduction to Nonlinear Optical Effect in Molecules and Polymers* (New York: Wiley, 1991).
3. M.S. Pandian, S. Verma, P. Karuppasamy, P. Ramasamy, V.S. Tiwari, and A.K. Karnal, Unidirectional crystal growth of L-alanine doped triglycine sulphate crystals along [010] polar direction in ferroelectric and paraelectric temperature ranges and their comparative characterizations. *Mater. Res. Bull.* 134, 111118 (2021).
4. D.A. Fentaw, M. Esthaku Peter, and T. Abza, Synthesis and characterization of lanthanum chloride doped L-alanine maleate single crystals. *J. Cryst. Growth* 522, 1 (2019).
5. Su. Narmatha, R. Surekha, and K. Ambujam, Synthesis-spectroscopic, optical and thermal properties of L-alanine ammonium chloride—a semiorganic crystal. *Optik* 125, 6826 (2014).
6. R. Ravisankar, P. Jayaprakash, and P. Eswaran, Synthesis, growth, optical and third-order nonlinear optical properties of glycine sodium nitrate single crystal for photonic device applications. *J. Mater. Sci. Mater. Electron.* 31, 17320 (2020).
7. S. Thangavel, V. Kathiravan, R. Ashok Kumar, S. Eniya, G. Satheesh Kumar, P. Selvarajan, and M. Kumaresavanji, Crystal growth of L-alanine oxalic acid crystal and its spectral, NLO, mechanical, thermal, and impedance properties. *J. Electron. Mater.* 51, 3068 (2022).
8. D.S. Chemla and J. Zyss, *Nonlinear Optical Properties of Organic Molecules and Crystals* (New York: Academic Press, 1987).
9. S. Thangavel, V. Kathiravan, R. Ashok Kumar, G. Satheesh Kumar, and P. Selvarajan, Spectral, optical, mechanical, impedance, and nonlinear optical properties of amaranth (dye)-doped L-histidine hydrochloride monohydrate crystal. *J. Mater. Sci. Mater. Electron.* 33, 12249 (2022).
10. N. Suresh and M. Selvapandiyan, Influence of zirconium nitrate doping on the properties of L-alanine crystal for nonlinear optical applications. *J. Mater. Sci. Mater. Electron.* 31, 16737 (2020).
11. M. Delfino, A comprehensive optical second harmonic generation study of the non-centrosymmetric character of biological structures. *Mol. Cryst. Liq. Cryst.* 52, 271 (1979).

12. K. Kirubavathi, K. Selvaraju, R. Valluvan, N. Vijayan, and S. Kumararaman, Synthesis, growth, Structural, spectroscopic, and optical studies of a new semi-organic nonlinear optical crystal: L-valine hydrochloride. *Spectrochim. Acta A* 69, 1283 (2008).
13. M.S. Rajamudhideen, K. Sethuraman, K. Ramamurthi, and P. Ramasamy, Growth and physical characterization of organic nonlinear optical single crystal: N, N-diphenyl guanidinium formate. *Opt. Laser Technol.* 91, 159 (2017).
14. M. Thangaraj, G. Ravi, T. Binitha, and A. Loganathan, Ethylene diammonium di (4-nitrophenolate): a third order NLO material for optical limiting. *Spectrochim. Acta A* 138, 158 (2014).
15. S. Thangavel, V. Kathiravan, R. Ashok Kumar, S. Eniya, G. Satheesh Kumar, P. Selvarajan, and M. Kumaresavanji, Studies on growth and characterization of a nonlinear optical crystal: zinc sulfate-doped L–alanine. *J. Nonlinear Opt. Phys. Mater.* 6, 2350024 (2022).
16. K. Mohanraj, D. Balasubramanian, and N. Jhansi, Growth, structural and optical properties of novel nonlinear optical potassium phthalate di lithium borate (KPDLiB) single crystals. *Mater. Sci. Pol.* 38, 214 (2020).
17. V. Kathiravan, G. Satheesh Kumar, S. Pari, and P. Selvarajan, Influence of dye doping on the structural, spectral, optical, thermal, electrical, mechanical and nonlinear optical properties of L-histidine hydrofluoride dihydrate crystals. *J. Mol. Struct.* 1223, 128958 (2021).
18. I. Cicili Ignatius, S. Rajathi, K. Kirubavathi, and K. Selvaraju, Studies on growth and characterization of L-alanine strontium chloride trihydrate single crystals for optical applications. *Optik* 125, 4265 (2014).
19. S. Krishnan, C. Justin Raj, S. Dhinakaran, and S. Jerome Das, Investigation of optical bandgap in potassium acid phthalate single crystal. *Cryst. Res. Technol.* 43, 670 (2008).
20. D. Rajan Babu, D. Jayaraman, R. Mohan Kumar, and R. Jayavel, Growth and characterization of nonlinear optical L-alanine tetrafluoroborate (L-AIFB) single crystals. *J. Cryst. Growth* 245, 121 (2008).
21. C. Justin Raj and S. Jerome Das, Growth and characterization of nonlinear optical active L-alanine formate crystal by modified Sankaranarayanan-Ramasamy (SR) method. *J. Cryst. Growth* 304, 191 (2007).
22. A.S.J. Lucia Rose, P. Selvarajan, and S. Perumal, Studies on growth and characterization of an NLO crystal: L-alanine hydrogen chloride (LAHC). *Mater. Chem. Phys.* 130, 950 (2011).
23. G. Anandha Babu, R. Perumal Ramasamy, and P. Ramasamy, Synthesis, crystal growth and characterization of an efficient nonlinear optical D–π–A type single crystal: 2-aminopyridinium 4-nitrophenolate 4-nitrophenol. *Mater. Chem. Phys.* 117, 326 (2009).
24. M. Lydia Caroline, R. Sankar, R.M. Indirani, and S. Vasudevan, Growth, optical, thermal and dielectric studies of an amino acid organic nonlinear optical material: L-alanine. *Mater. Chem. Phys.* 114, 490 (2009).
25. N. Vijayan, S. Rajasekaran, G. Bhagavannarayana, R. Ramesh Babu, R. Gopalakrishnan, and M. Palanichamy, *Cryst. Growth Des.* 6, 2441 (2006).
26. C. Razzetti, M. Arduino, L. Zanotti, M. Zha, and C. Parorici, Solution growth and characterization of L-alanine single crystals. *Cryst. Res. Technol.* 37, 456 (2002).
27. C. Ramachandra Raja, G. Gokila, and A. Antony Joseph, Growth and spectroscopic characterization of a new organic nonlinear optical crystal: L- alaninium succinate. *Spectrochim. Acta Part A* 72, 753 (2009).
28. B.K. Periyasamy, R.S. Jebas, N. Gopalakrishnan, and T. Balasubramanian, Development of NLO tunable band gap organic devices for optoelectronic applications. *Mater. Lett.* 61, 4246 (2007).
29. D. Shanthi, P. Selvarajan, and S. Perumal, Growth, linear optical constants and photoluminescence characteristics of beta-alaninium picrate (BAP) crystals. *Optik* 127, 3192 (2016).
30. K.A. Aly, Comment on the relationship between electrical and optical conductivity used in several recent papers published in the journal of materials science: materials in electronics. *J. Mater. Sci. Mater. Electron.* 33, 2889 (2022).
31. V. Gupta and A. Mansingh, Influence of post-deposition annealing on the structural and optical properties of the sputtered zinc oxide film. *J. Appl. Phys.* 80, 1063 (1996).
32. P. Pandi, G. Peramaiyan, G. Bhagavannarayana, R. Mohan Kumar, and R. Jayavel, Growth, structural, optical, and laser damage threshold studies of organic picolinium picrate monohydrate single crystals. *Optik* 124, 5792 (2013).
33. F. Yakuphanoglu and H. Erten, Refractive index dispersion, and analysis of the optical constants of an ionomer thin film. *Opt. Appl.* 35, 969 (2005).
34. M.A. Gaffar, A. Abu El-Fadl, and S. Bin Anooz, Influence of strontium doping on the indirect bandgap and optical constants of ammonium zinc chloride crystals. *Phys. B Condens. Matter* 327, 43 (2003).
35. P. Sathya, M. Anantharaja, N. Elavarasu, and R. Gopalakrishnan, Growth and characterization of nonlinear optical single crystals: bis(cyclohexylammonium) terephthalate and cyclohexylammonium para-methoxy benzoate. *Bull. Mater. Indian Acad. Sci. Sci.* 38, 1291 (2015).
36. S.S. Kurtz and T. Perry, A powder technique for the evaluation of nonlinear optical materials. *J. Appl. Phys.* 39, 3798 (1968).
37. K. Sethuraman, R. Ramesh Babu, R. Gopalakrishnan, and P. Ramasamy, Synthesis, growth, and characterization of a new semiorganic nonlinear optical crystal: L-alanine sodium nitrate (LASN). *Cryst. Growth Des.* 8, 1863 (2008).
38. E.M. Onitsch, *Mikroskopie* 2, 131 (1947).
39. L. Misoguti, A.T. Varela, F.D. Nunes, V.S. Bagnato, F.E.A. Melo, F.J. Mendes, and S.C. Zilio, *Opt. Mater.* 6, 147 (1996).
40. K. Li, X. Wang, and D. Xue, *Mater. Focus* 1, 142–148 (2012).
41. K. Li, X. Wang, F. Zhang, and D. Xue, *Phys. Rev. Lett.* 100, 235504 (2008).
42. R. Surekha, R. Gunaseelan, P. Sagayaraj, and K. Ambujam, *R. Soc. Chem.* 16, 7979 (2014).
43. T. Balakrishnan and K. Ramamurthi, Growth, structural, optical, thermal and mechanical properties of glycine zinc chloride single crystal. *Mater. Lett.* 62, 65 (2008).
44. A. Abu El-Fad, J.A.S. Soltan, and N.M. Shaala, Influence of X-irradiation on indentation size effect and formation of cracks for $[K_y (NH_4)_{1-y}]_2 ZnCl_4$ mixed crystals. *Cryst. Res. Technol.* 42, 364 (2007).
45. W. Mott, A. Ramanand, and D. Jayaraman, *Optoelectron. Adv. Mater.* 4, 1987 (2010).
46. D. Shanthi, P. Selvarajan, and R. Jothi Mani, Nucleation kinetics, growth and hardness parameters of L-alanine alaninium picrate (LAAP) single crystals. *Optik* 125, 2531 (2014).
47. P. Jayaprakash, M. Peer Mohamed, P. Krishnan, M. Nageshwari, G. Mani, and M. Lydia Caroline, *Phys. B* 503, 25 (2016).
48. F.Q. Meng, M.K. Lu, Z.H. Yang, and H. Zeng, Thermal and crystallographic properties of a new NLO material, urea-(d) tartaric acid single crystal. *J. Mater. Lett.* 33, 265 (1998).
49. D. Shanthi, P. Selvarajan, and S. Perumal, Growth, spectral, third order NLO and impedance analysis of L-alaninium maleate crystals admixtured with urea. *Mater. Today Proc.* 2, 943 (2015).
50. K.V. Rajendran, D. Jayaraman, R. Jeyavel, R. Mohan Kumar, and P. Ramasamy, Growth and characterization of nonlinear optical L-histidine tetrafluoroborate (L-HFB) single crystals. *J. Cryst. Growth* 224, 122 (2001).

51. R.N.P. Subhadarsani Sahoo, and B.K.M. Choudhary, Structural, ferroelectric and impedance spectroscopy properties of Y^{3+} modified Pb ($Fe_{0.5}$ $Nb_{0.5}$)O_3 ceramics. *Phys. B* 406, 1660 (2011).
52. K. Li, P. Yang, L. Niu, and D. Xue, *J. Phys. Chem. A* 116, 6911 (2012).